Particle-hole strength excited in the ^{48}Ca(p,n)^{48}Sc reaction at 134 and 160 MeV: $(\pi f_{7/2}, \nu f^{-1}_{7/2})$ band

B. D. Anderson, T. Chittrakarn, A. R. Baldwin, C. Lebo, R. Madey, R. J. McCarthy, and J. W. Watson

Department of Physics, Kent State University, Kent, Ohio 44242

B. A. Brown

Cyclotron Laboratory, Michigan State University, East Lansing, Michigan 48824

C. C. Foster

Indiana University Cyclotron Facility, Bloomington, Indiana 47405

The ^{48}Ca(p,n)^{48}Sc reaction was studied at 134 and 160 MeV. Neutron energy spectra were measured by the time-of-flight technique with resolutions from 320 to 460 keV at 11 angles from 0° to 60° spaced approximately 6° apart. The neutron spectra reveal strong excitation of the $(\pi f_{7/2}, \nu f^{-1}_{7/2})$ band of states at low excitation energies; five of the known eight members of the band are excited strongly, generally consistent with distorted-wave-impulse-approximation calculations with $1f$-$2p$ shell-model wave functions. The normalization of the distorted-wave-impulse-approximation calculations to the extracted angular distributions at 135 MeV vary from 0.40 for the 5^+ state to 0.93 for the 0^+, isobaric analog state. The normalization factor of 0.60 required for the 7^+, stretched-state transition is significantly larger than those required for similar distorted-wave-impulse-approximation calculations of various stretched-state excitations observed in inelastic proton scattering, which involve promoting a nucleon up into the next major shell (a "1 $\hbar\omega$" excitation). The larger normalization factor required for the $(\pi f_{7/2}, \nu f^{-1}_{7/2})$ 7^+ excitation (a "0 $\hbar\omega$" excitation) indicates that this strength is more highly concentrated in a single state. The 4^+ and 6^+ states of this band are observed to be only weakly excited, consistent with predictions that transitions dominated by the tensor term of the nucleon-nucleon interaction will predominantly excite non-normal parity states. The excitation of the 2^+ member of this band shows both $\Delta l = 0$ and $\Delta l = 2$ contributions to the angular distribution and may indicate significant two-step processes for this transition.

I. INTRODUCTION

The (p,n) reaction at medium energies can be described well as a one-step, impulsive process;[1-3] accordingly, the (p,n) reaction on good closed-shell target nuclei excites predominantly one-particle—one-hole states. Such excitations are *relatively* easy to describe theoretically and comparisons with experimental results can provide important tests of both nuclear structure and reaction mechanism models. Because ^{48}Ca is believed to be one of the best examples of a good closed-shell nucleus, the ^{48}Ca(p,n)^{48}Sc reaction is expected to provide some of the best tests of these models.

In an earlier study[3] of the (p,n) reaction on ^{16}O, all of the strongest excitations were described well by a combination of a shell-model calculation[4] in the Tamm-Dancoff approximation (TDA) and a distorted-wave-impulse-approximation (DWIA) model of the reaction mechanism. These results were somewhat surprising because multiparticle-multihole correlations in the ^{16}O ground state might be expected to yield large amounts of more complicated configurations for final states excited in the (p,n) reaction. The good agreement obtained indicates that the most strongly-excited states *are* relatively good particle-hole states and that the (p,n) reaction at medium energies predominantly excites such states. The ^{48}Ca(p,n)^{48}Sc reaction provides two important advantages

over the ^{16}O(p,n)^{16}F reaction for further quantitative analyses of particle-hole excitations. First, the ^{48}Ca ground state is believed to involve fewer correlations, so that there is a better theoretical basis for expecting particle-hole states to be less mixed with multiparticle-multihole configurations. Second, the ^{48}Ca nucleus has eight excess neutrons; hence, the (p,n) charge-exchange reaction can excite (in ^{48}Sc) the known[5,6] $(\pi f_{7/2}, \nu f^{-1}_{7/2})$ particle-hole band of states, including the analog of the target ground state. This band provides a spectrum of states which can test both structure models and reaction mechanisms in a relatively simple manner.

After presenting the experimental results, we analyze first the transitions to the 0^+ isobaric analog state (IAS) of the ^{48}Ca-target ground state and to the 7^+ "stretched state." Because the 0^+, IAS transition presumably is between two states of nearly identical nuclear structure, complete overlap of the initial- and final-state wave functions can be assumed. Thus, the IAS transition provides a test of the reaction-mechanism model, viz., the assumption of a one-step, impulsive reaction, the distorted-wave descriptions, and the strength of the isospin-transfer strength in the nucleon-nucleon effective interaction used in the microscopic calculations. The 7^+ transition is to the highest spin member of the $(f_{7/2}, f^{-1}_{7/2})$ particle-hole octet which can be excited via a charge-exchange reaction on the excess neutrons in ^{48}Ca. This structure is unique

for a 7^+ state in a 1p-1h basis within 2 $\hbar\omega$ of excitation; the analysis of the strength of this transition, therefore, addresses the strength of the appropriate term in the effective interaction (viz., the tensor term as discussed below), *and* the closed-shell assumption for the target nucleus.

Finally, we consider the excitation of the other members of the $(f_{7/2}, f_{7/2}^{-1})$ particle-hole band in ^{48}Sc; their excitation energies are available in the literature. The structure of these intermediate states is neither identical to the target nucleus nor unique within a large range of excitation energies, but their excitations can be compared with DWIA calculations using $1f$-$2p$ shell-model wave functions. The excitation of these intermediate states necessarily involves varying degrees of central, spin orbit, and tensor strength in the nucleon-nucleon effective interaction used to describe the reactions. In a companion paper, we discuss the excitation of the 1^+, so-called Gamow-Teller (GT), strength observed in this reaction.

II. EXPERIMENTAL PROCEDURE

The experimental measurements were performed at the Indiana University Cyclotron Facility (IUCF) with the beam-swinger system.[7] Neutron energies were measured by the time-of-flight technique. The measurements at 135 and 160 MeV were performed in separate experimental runs. Initial results from the 160 MeV measurements were reported earlier.[1,8] For both energies, neutrons were detected in large-volume, mean-timed neutron detectors[9] with overall time dispersions of 0.5 to 0.7 ns. Neutron time of flight was measured relative to the arrival of the beam on the target, which was derived from a point of fixed phase of the cyclotron rf signal. A phase-compensation circuit[10] was used to reduce drift between the time of arrival of a beam burst on the target and the cyclotron rf signal. A fast plastic scintillator monitored elastically-scattered protons from the target to provide the necessary timing information to the phase-compensation circuit. The neutron detectors were all 10.2 cm thick by 1.02 m or 1.52 m long, with heights of 25.4, 50.8, 76.2 cm, or 1.02 m. The basic experimental procedure was described previously.[3]

For the 135 MeV measurements, neutron detectors were placed in three detector stations at 0°, 24°, and 45° with respect to the undeflected beam. Two 1.02 m long by 50.8 cm high neutron detectors were used in the 0° station at a flight path of 71.0±0.2 m. One 50.8 cm high detector plus one 1.02 m high detector, both 1.02 m long, were used in the 24° station, also at a flight path of 71.0±0.2 m. Two 76.2 cm high by 1.52 m long neutron detectors were used in the 45° detector station at a flight path of 37.3±0.2 m. Thin (0.95 to 1.27 cm thick) scintillator detectors were placed in front and on top of the neutron detectors to veto charged particles from the target and most cosmic rays. Overall time dispersions of about 0.7 ns were observed which yield energy resolutions of about 320 keV in the two forward-angle detector stations and about 450 keV in the widest-angle station.

For the 160 MeV measurements, neutron detectors were placed in two detector stations at 0° and 24° with respect to the undeflected beam in the swinger system. Two 1.02 m long by 25.4 cm high detectors were used in the 0° station at a flight path of 68.0±0.2 m from the target. One 25.4 cm high detector plus one 50.8 cm high detector, both 1.02 m long, were used in the 24° station at a flight path of 76.3±0.2 m. Intermediate angles and angles out to 48.5° were studied by deflecting the incident proton beam at the target with the beam-swinger system. Thin (0.6 cm) scintillator detectors were placed in front and on top of the neutron detectors to veto charged particles from the target as well as most cosmic rays. Overall time dispersions of about 0.5 ns were obtained. These time dispersions included contributions not only from the intrinsic time dispersions of the neutron detectors, but also from the burst width of the beam, the beam energy spread, and the beam energy loss in the target. The observed time dispersions combine with the measured flight paths to yield neutron energy resolutions of about 450 keV in the 0° detector station and about 400 keV in the 24° detector station.

Absolute cross sections for various specific transitions were extracted from the known target thickness, measured geometry, charge-integrated beam, and calculated neutron detector efficiencies. The calcium target was enriched to 97.3% and contained 28.5±0.5 mg/cm^2 of ^{48}Ca. The target thickness was determined with a "ball" micrometer and checked by weighing. The principal contaminant was 2.6% ^{40}Ca. The target was prepared and stored in vacuum and transferred in an inert atmosphere. The later (135 MeV) experimental run showed evidence of some oxidation ($\sim$5% by weight). The proton beam intensity was measured with a split Faraday cup, which was well shielded and located approximately 10 m downstream from the target. The beam integration was estimated to be accurate to $\lesssim \pm 5\%$. The largest geometrical uncertainty is in the measured flight paths which are estimated to be known to ±0.2 m. This flight-path uncertainty corresponds to a maximum uncertainty of ±1.0% in the known solid angle (for the shortest flight path).

In order to determine reliably the neutron detector efficiencies, it was necessary to calibrate the pulse-height response of each detector, which was performed with a ^{232}Th radioactive gamma-ray source ($E_\gamma = 2.61$ MeV) and a calibrated fast amplifier. This method was checked during the 160 MeV run to be accurate to $\sim \pm 3\%$ by comparison with pulse heights observed for 99 MeV protons scattered elastically into the neutron detector.[9]

The neutron detector efficiencies were calculated with the Monte Carlo code of Cecil *et al.*[11] This computer code is an improved version of the earlier codes of Stanton[12] and of McNaughton *et al.*[13] The improved version uses relativistic kinematics, properly determines light output for escaping charged particles, and includes an adjustment of the cross sections for the single most important reaction channel at neutron energies above 30 MeV, viz., the ^{12}C(n,p)X reaction. The adjustments were performed to provide better agreement with several separate measurements of neutron detector efficiencies. The basic result was that the cross sections for this reaction were reduced between about 30 and 90 MeV from those adopted in the earlier versions of this code. The reduction of these cross

sections was subsequently verified by experimental measurements[14] of the reaction cross sections for neutrons on carbon near 60 MeV.

The calculated efficiencies for the large-volume neutron detectors used in the experiments at the IUCF were tested experimentally.[15,16] Measured (p,n) cross sections on self-conjugate targets to known ($T = 1$) analog states can be compared with measured (p,p') cross sections to the parent states. In the limit of no isospin mixing, the cross section ratio is determined by simple isospin Clebsch-Gordan coefficients to be $\sigma(p,n)/\sigma(p,p') = 2$. Coulomb energy shifts which can alter the kinematics and different distorting potentials in the exit channels prevent this relationship from being exact; however, theoretical DWIA calculations indicate that these effects are small ($\lesssim 5\%$) for the incident energies considered here. Comparisons were performed for the transitions to the $T = 1$, 4^-, and 6^- stretched states excited by 135 MeV protons on targets of ^{16}O and ^{28}Si, respectively, as well as to the strongly-excited 1^+, "Gamow-Teller" ground state in ^{12}N by 120, 135, and 160 MeV protons on carbon. All of these states are believed to be relatively pure $T = 1$ isospin states, and the (p,n) to (p,p') cross section ratios are all observed to be the expected value of two, to within the combined experimental uncertainties ($\sim \pm 12\%$). Also, the value of the $^{12}C(p,n)^{12}N(1^+,g.s.)$ cross section at 144 MeV was measured by Moake et al.[17] with neutron detector efficiencies determined by an associate-particle measurement. Their result agrees with our measured values (at 135 and 160 MeV) to better than 10% (which is less than their stated systematic uncertainty). These various tests of the calculated efficiencies are described in more detail elsewhere.[16]

Because the Monte Carlo calculated efficiencies provide (p,n) cross sections in good agreement with several separate analog (p,p') cross sections, as well as with an independent measurement of the $^{12}C(p,n)^{12}N$ g.s. cross section, and because the Monte Carlo calculations provide good agreement with several available neutron detector efficiency measurements, we accept the Monte Carlo calculations as accurate to better than ±10%. (Note that this uncertainty includes a contribution from the uncertainty in the pulse-height threshold set on each detector as discussed below.)

III. DATA REDUCTION

The data were recorded during the experimental runs event-by-event in two parameters for each neutron detector. Both the neutron time of flight and the detector pulse height were recorded for each event. The event tapes were later reread at various pulse-height thresholds in order to extract time-of-flight spectra, excitation-energy spectra, and cross sections.

Excitation-energy spectra were obtained from the measured time-of-flight spectra by using the known flight path and the calibration of the time-to-amplitude converter (TAC). Known[6] excitation energies of states in ^{48}Sc were taken to provide the absolute calibration of neutron energies. At forward angles, the strongly-excited 1^+ state at $E_x = 2.52$ MeV and the 0^+, IAS at $E_x = 6.67$ MeV were taken to provide this calibration; and at wide angles,

the 7^+ state at $E_x = 1.096$ MeV was used. The locations of other known peaks were then checked in order to confirm these calibrations, as discussed more fully below. Excitation-energy spectra derived from the 135 and 160 MeV data are presented in Figs. 1 and 2, respectively.

Cross sections for individual transitions were obtained by summing the events under the peaks and/or by "fitting" the peaks in the time-of-flight spectra. The peak sums were then combined with the known target thickness, detector solid angles, the calculated detector efficiencies, and the measured beam integration to obtain differential cross sections. These cross sections were corrected for system dead-time and neutron attenuation in the target-chamber wall and the air. The overall systematic uncertainty is estimated to be ±12%, which includes contributions from the neutron detector efficiency (±10%), the proton-beam integration (±5%), the neutron attenuation (±5%), the target thickness (±2%), and the system dead-time correction (±1%).

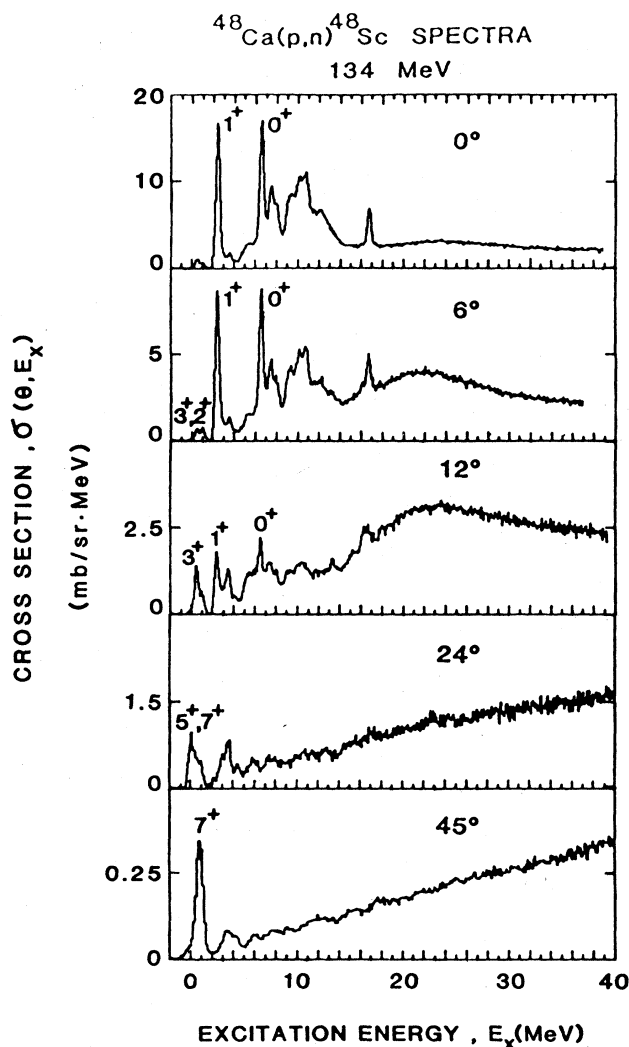Please note that the 160 MeV cross sections presented here differ by about 40% from those presented earlier.[1]

FIG. 1. Neutron excitation-energy spectra from the $^{48}Ca(p,n)^{48}Sc$ reaction at 134 MeV.

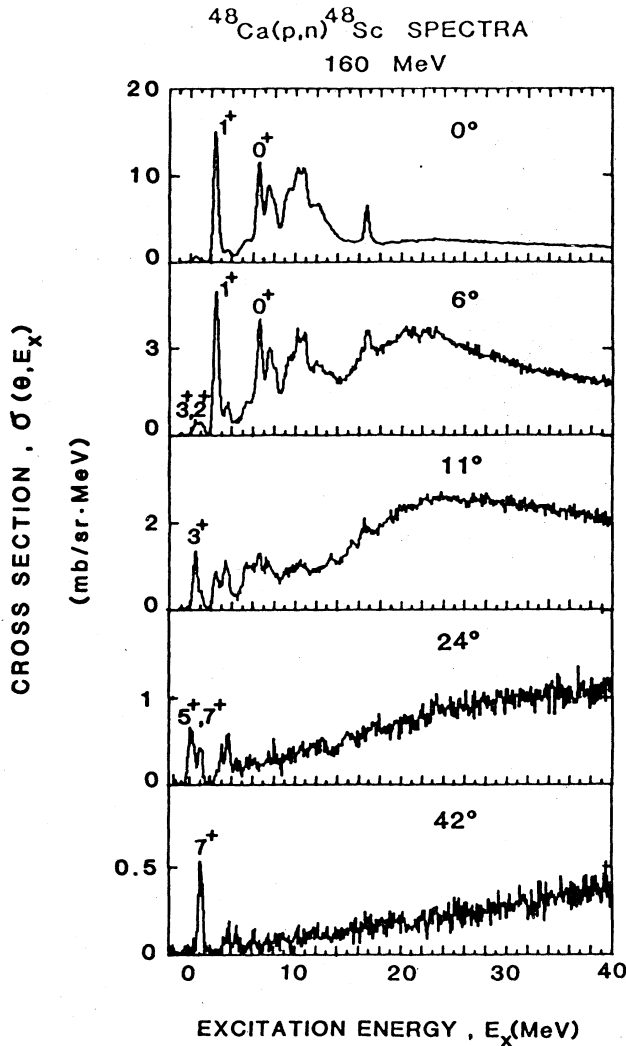FIG. 2. Neutron excitation-energy spectra from the ^{48}Ca(p,n)^{48}Sc reaction at 160 MeV.

separate regions. The region below the Gamow-Teller giant resonance (from $E_x = 5$ to 14 MeV) is dominated by transitions to members of the $(f_{7/2}, f_{7/2}^{-1})$ particle-hole octet and is observed to be composed of two complexes, one between $0 \leq E_x(\text{MeV}) \lesssim 1$, and the other between $2.5 \lesssim E_x(\text{MeV}) \lesssim 4$. Since both of these complexes are composed of bound states in ^{48}Sc, the widths of the states should be entirely instrumental and equal; therefore, the peaks in each complex were fit simultaneously with Gaussian peaks always required to have equal widths. (Note that the width can vary from detector to detector and for different runs.) Examples of the Gaussian peak-fitting results of the 0 to 1 MeV complex are shown in Fig. 3. Because states become unbound in ^{48}Sc near $E_x = 9$ MeV, the Gamow-Teller giant resonance (GTGR) from $4.5 \leq E_x(\text{MeV}) \leq 14.5$ was fit with peaks which were allowed to vary in width. The fit to this complex at 0° is shown in Fig. 4. Because the exact number of levels in this complex is not known, the complex was fit with the minimum number of peaks required to obtain a good fit. The background assumed here is a simple quadratic polynomial and was fit simultaneously with the peaks. This choice of background is sometimes called an
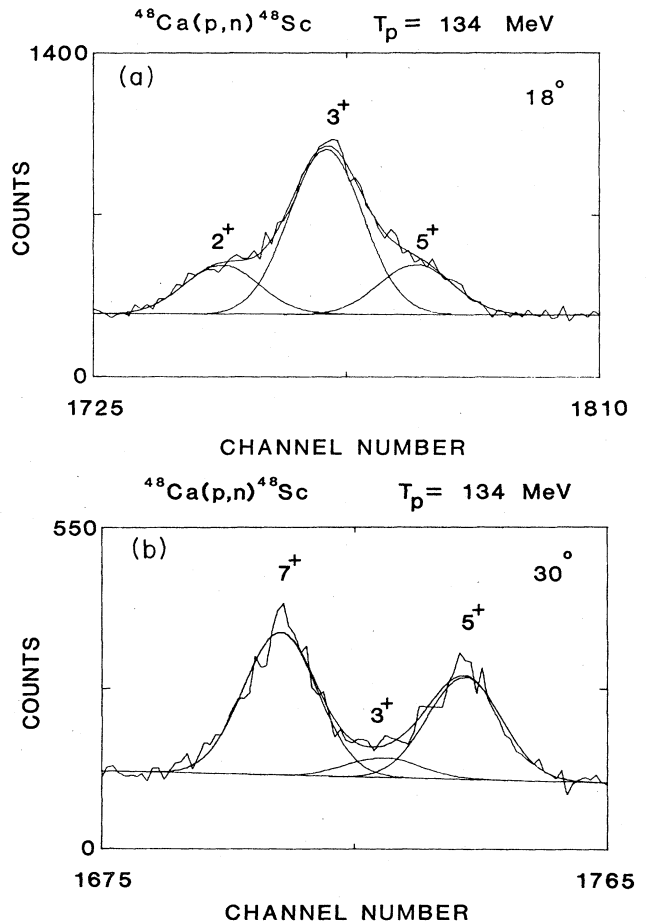

FIG. 3. Examples of the Gaussian-fitting results at (a) 18° and (b) 30° for the low-lying complexes of states in the ^{48}Ca(p,n)^{48}Sc reaction at 134 MeV (see the text for details).

This difference occurs because of an inadvertent omission (in the earlier results) of the correction for neutron attenuation in a 2.22 cm thick copper plate which we used in the 160 MeV run to ensure that charged particles from the target could not be detected by the neutron counters. (The charged-particle anticoincidence counters were only 0.6 cm thick and were suspected to be $< 100\%$ efficient for that run.) This copper plate was used only for the 160 MeV ^{48}Ca experimental run and was neglected only in the paper of Anderson *et al.*[1] [The later paper by Watson *et al.*[8] reporting the observation of the "0 $\hbar\omega$," 7^+ state excitation in the ^{48}Ca(p,n)^{48}Sc reaction at 160 MeV *did* include a correction for the neutron attenuation in the copper plate.] No other experimental results reported by the various Kent State University collaborations are affected by this correction.

The yields of separate transitions were extracted with an improved version of the peak-fitting code of Bevington.[18] Basically, the (p,n) spectrum was fit in two

^{48}Ca(p,n)^{48}Sc T_p = 134 MeV
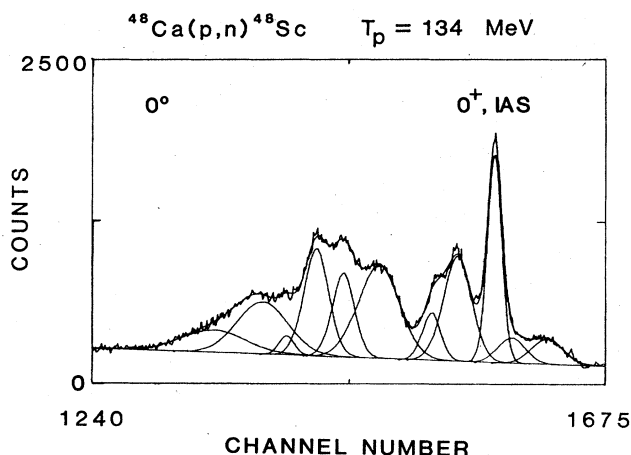
FIG. 4. The Gaussian-fitting results at 0° for the Gamow-Teller giant resonance (GTGR) region in the ^{48}Ca(p,n)^{48}Sc reaction at 134 MeV. The fitted 0$^+$, IAS included in the complex of states is indicated.

"experimentalist's background." Osterfeld[19] indicated that much of this experimentalist's background may include 1$^+$, Gamow-Teller strength. We discuss this question in the companion paper. We note that the background shown in Fig. 4 permits extracting the cross sections for the individual, strongly-excited states. Note especially that one of these states is the 0$^+$, IAS at $E_x = 6.67$ MeV, which needs to be extracted reliably from the other (presumably 1$^+$) strength observed in this complex. Because enough of the 0$^+$, IAS is observed above the background of other states, it fits well at both 135 and 160 MeV. It is not important, for the present work, if some of the peaks indicated in Fig. 4 are actually unresolved complexes, since all of this strength is peaked at 0° and will be interpreted to be 1$^+$ strength, as described in the companion paper.

For the transitions considered in this paper, the extracted peak areas are determined well by the fitting program. The backgrounds for the 0 to 1 MeV complexes are flat and well determined. Although the 0$^+$, IAS state is in the middle of the 1$^+$ complex of states, it stands out sufficiently to be determined well and is not sensitive to the choice of the fitted background. The uncertainties shown in the angular distributions of Figs. 5–10 are from the error matrix of the fitting program[18] and are primarily statistical. All of the results are subject to the overall systematic uncertainty of $\sim \pm 12\%$ as well, as discussed above.

IV. RESULTS AND DISCUSSION

As indicated earlier, we present and discuss the results in an order which addresses first the validity of assuming one-step, impulsive reaction mechanisms by considering transitions to states of relatively well-known nuclear structure, and then proceed to consider transitions to the states with more complicated structures. Thus, we consider first the transitions to the 0$^+$, IAS and the 7$^+$,

stretched state, and then consider the transitions to the other members of the $(f_{7/2}, f_{7/2}^{-1})$ particle-hole band.

A. The 0$^+$, IAS transition

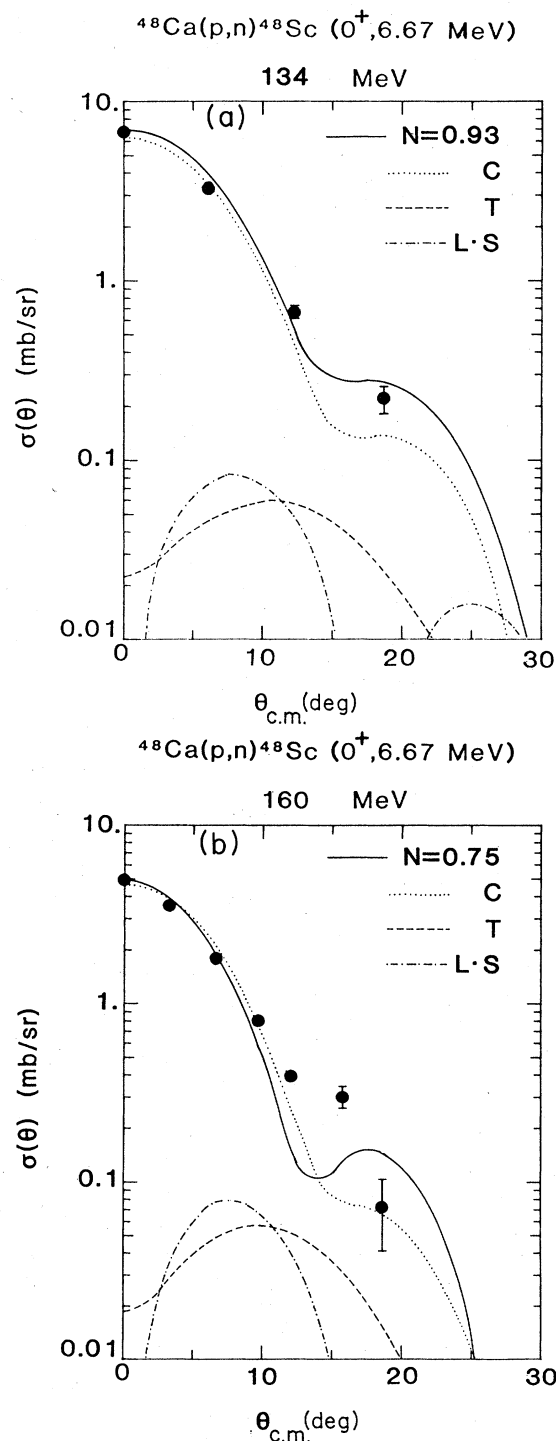The experimental angular distributions for the transition to the 0$^+$, isobaric analog state are presented in Fig.

FIG. 5. Angular distributions at (a) 134 and (b) 160 MeV for the ^{48}Ca(p,n)^{48}Sc reaction to the 0$^+$ (IAS), 6.67 MeV state. The curves represent DWIA calculations as described in the text.
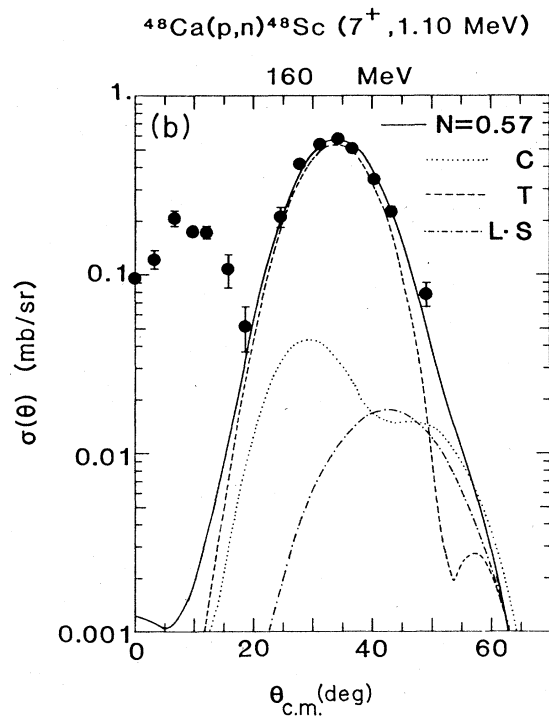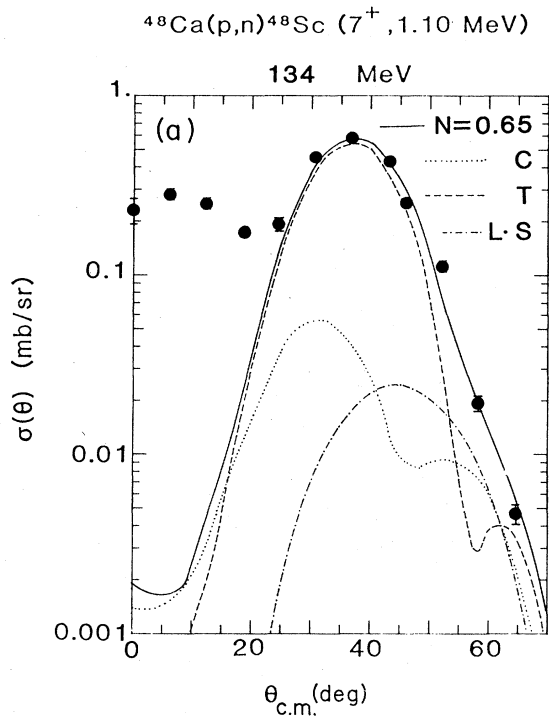
^{48}Ca(p,n)^{48}Sc (7$^+$,1.10 MeV)

^{48}Ca(p,n)^{48}Sc (1$^+$,2.52 MeV)

^{48}Ca(p,n)^{48}Sc (7$^+$,1.10 MeV)

^{48}Ca(p,n)^{48}Sc (1$^+$,2.52 MeV)

FIG. 6. Angular distributions at (a) 134 and (b) 160 MeV for the ^{48}Ca(p,n)^{48}Sc reaction to the 7$^+$ (0 $\hbar\omega$ stretched state), 1.10 MeV complex. The curves represent DWIA calculations as described in the text.

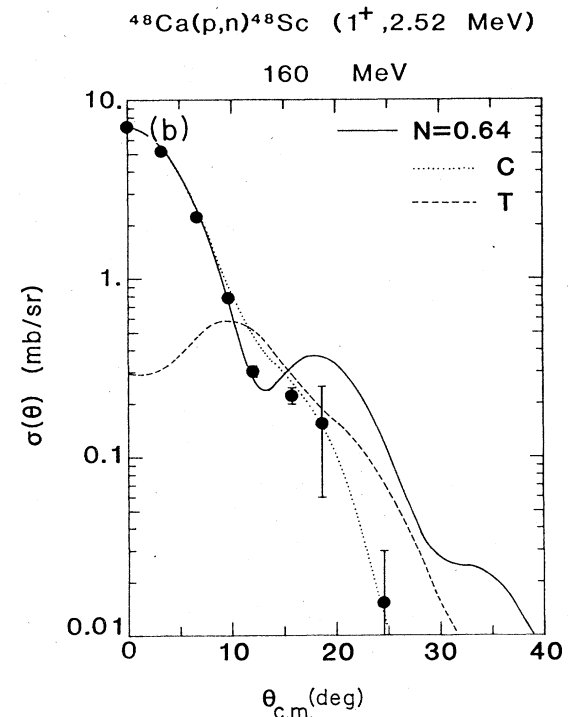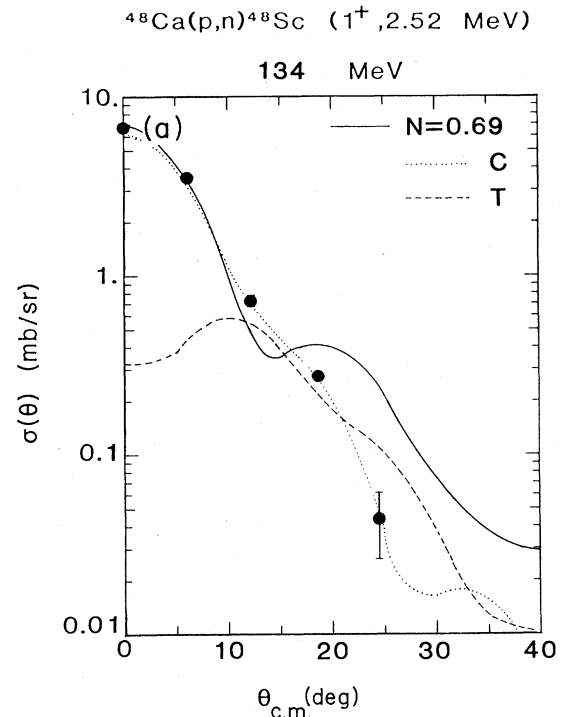FIG. 7. Angular distributions at (a) 134 and (b) 160 MeV for the ^{48}Ca(p,n)^{48}Sc reaction to the 1$^+$, 2.52 MeV state. The curves represent DWIA calculations as described in the text.

5. This state at $E_x = 6.67$ MeV is known[6] to be the analog of the ground state of the ^{48}Ca target. The strength for this state was extracted by fitting the Gamow-Teller giant resonance (GTGR) region between $4.5 \leq E_x(\text{MeV}) \leq 14.5$

as illustrated in Fig. 4 and described in Sec. III. The structure of the final state (in ^{48}Sc) is essentially identical to that of the target. Shown also in Fig. 5 are distorted-wave impulse-approximation (DWIA) calculations for this
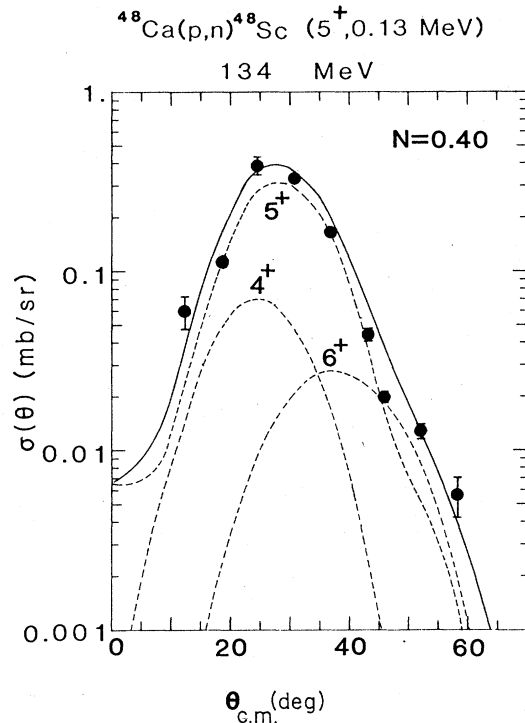
^{48}Ca(p,n)^{48}Sc (5$^+$,0.13 MeV)

134 MeV

N=0.40

^{48}Ca(p,n)^{48}Sc(3$^+$,0.622 MeV)

134 MeV

N=0.45 ——
C ········
T - - - -

FIG. 8. Angular distribution at 134 MeV for the ^{48}Ca(p,n)^{48}Sc reaction to the 4$^+$, 5$^+$, 6$^+$ complex at 0.1 MeV. The curves represent DWIA calculations as described in the text.
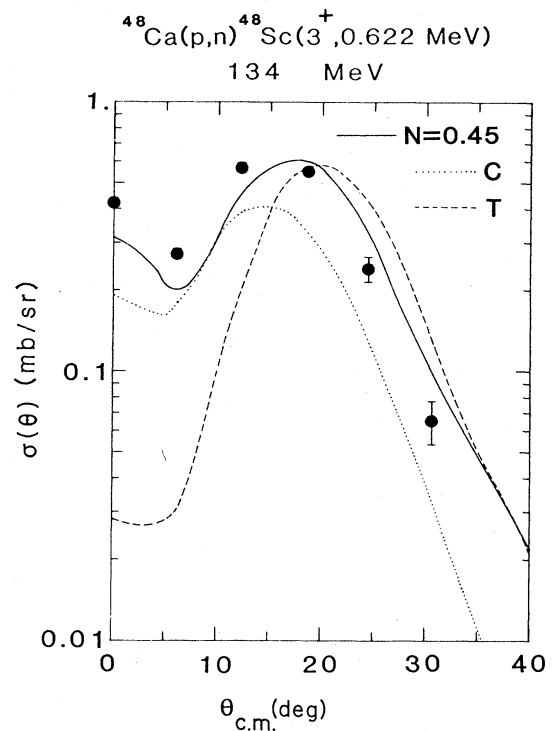
FIG. 9. Angular distribution at 134 MeV for the ^{48}Ca(p,n)^{48}Sc reaction to the 3$^+$, 0.62 MeV state. The curves represent DWIA calculations as described in the text.

reaction. This calculation was performed with the code DWBA 70.[20] The optical-model parameters for the distorted waves were taken from the global parameters of Schwandt et al;[21] the nucleon-nucleon effective interaction assumed is that of Love and Franey[22] at 140 MeV; and the structure is assumed to be a pure $(\pi f_{7/2}, \nu f_{7/2}^{-1})$ configuration. Woods-Saxon potential-well wave functions were employed, with geometrical parameters taken from the work of Brown et al.[23] We used a fixed set of radial wave functions which were chosen to reproduce the single-particle separation energies between ^{47}Ca, ^{49}Ca, and ^{49}Sc, relative to ^{48}Ca. The agreement between the calculated and experimentally measured angular distributions is seen to be good, and the normalization factor is near unity for the 134 MeV measurements, but about 0.75 at 160 MeV.

The good agreement observed at 134 MeV between the calculated and measured angular distributions for the 0$^+$, IAS transition indicates several things. There are various ingredients in the calculations which directly affect the magnitude of the results. This transition is dominated by the so-called "Fermi" term which is the isospin-transfer, nonspin-transfer term of the nucleon-nucleon effective interaction. The calculated strength is directly proportional to the strength of the Fermi term in the effective interaction, which is taken to be that of Love and Franey[22] at 140 MeV. Secondly, the calculation assumes only a one-step, impulsive reaction, and neglects contributions to the strength from multistep processes. The incident and emitted particles are described by distorted waves, and the

magnitude of the calculated cross sections are sensitive to the net distortion. It is important to realize that these calculations are likely not sensitive to the assumed nuclear structure of the initial and final states. The ^{48}Ca target nucleus is known to be described relatively well as eight excess neutrons in the $f_{7/2}$ shell; furthermore, for this transition, there is good overlap of the initial and final state wave functions. Any deviations from the simple structure assumed for the ^{48}Ca target [viz., $(\nu f_{7/2})^8$], would be expected to affect this overlap only in second order.

The result that a factor of 0.75 is required to normalize the DWIA calculation to the experimental results at 160 MeV is almost certainly due to the use of the 140 MeV effective-interaction strength V_τ (Fermi) of Love and Franey. Taddeucci et al.[24] showed that the ratio $V_{\sigma\tau}/V_\tau$ (viz., the ratio of the spin-transfer, isospin-transfer term to the isospin-transfer term) must continue to increase from 140 to 200 MeV, whereas the effective interaction of Love and Franey indicates approximately the same value for this ratio at 140 and 200 MeV. (Our use of the 140 MeV value at 160 MeV is consistent with their indicated energy dependence.) As we will see below, the energy dependence of the $V_{\sigma\tau}$ term, from 140 to 200 MeV, is apparently constant (to within ~10%), so that it is the V_τ term which should be decreasing over this energy region. If we assumed a smaller value for V_τ at 160 MeV (say, from the observed ratio reported by Taddeucci et al.), we would obtain a normalization factor close to unity at 160 MeV also.
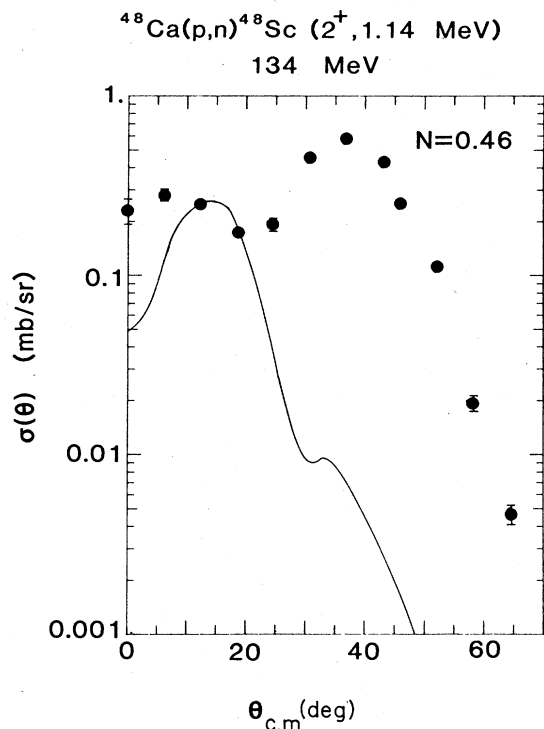
^{48}Ca(p,n)^{48}Sc (2$^+$,1.14 MeV)
134 MeV

FIG. 10. Angular distribution at 134 MeV for the ^{48}Ca(p,n)^{48}Sc reaction to the complex at 1.1 MeV. The curve represents DWIA calculations for a transition to a 2$^+$ state as described in the text.

The good agreement (especially at 134 MeV) between the calculated and experimental cross sections for the IAS transition appears to indicate that all of the basic ingredients are reasonable. Of course, it is possible that there are fortuitous compensating errors. Kelly and Carr[44] and also Auerbach *et al.*[45] found that a density-dependent N-N effective interaction may substantially affect the calculated IAS cross section. In our own studies, we find that use of "wine-bottle" optical potentials (which appear to fit some backward-angle elastic-scattering data better than simple Woods-Saxon potentials) will also affect the calculation; for example, we find that Stachler's[36] wine-bottle optical potential, which describes the elastic scattering data of 180 MeV protons on ^{40}Ca, reduces the calculated 0°, IAS cross section by 30%. Auerbach *et al.* find that using a density-dependent G matrix[46] reduces the calculated 0°, IAS cross section for the ^{90}Zr(p,n) reaction at 120 MeV by $\sim 35\%$ relative to a similar calculation using a free-nucleon G matrix. Auerbach *et al.* take the approach that one should find a combination of a density-dependent interaction and optical potentials which describe both the elastic scattering *and* the IAS cross section simultaneously; and find that they can succeed [at least for ^{90}Zr(p,n)]. In a sense, we have done this also, since the global optical parameters we have adopted should provide at least a reasonable description of the elastic scattering; however, since the uncertainties from these two considerations, as well as from other possible errors in the assumed reaction mechanisms, cannot be elim-

inated reliably at this time, the absolute spectroscopic factors reported here are probably uncertain by at least $\pm 30\%$.

B. The 7$^+$, "0 $\hbar\omega$" stretched-state transition

Next we consider the transition to the 7$^+$ state at $E_x = 1.10$ MeV in ^{48}Sc. This state, as discussed earlier, is the highest possible spin member of the $(f_{7/2}, f_{7/2}^{-1})$ octet of states. It is possible to make states of this spin with other one-particle, one-hole (1p-1h) configurations only by invoking excitations of 2 $\hbar\omega$ or greater. Thus, the 1p-1h structure of this final state is probably reliably known; furthermore, in contrast to most "1 $\hbar\omega$" stretched states excited in medium- or heavy-mass nuclei, the fact that both the particle and hole levels forming this state are at the Fermi surface of the nucleus means that these levels are not likely to be fragmented and that all of this particle-hole strength can be concentrated into one final state. Note that this 0 $\hbar\omega$ type of stretched state can be excited only in charge-exchange reactions because this state requires two nucleons to be in identical quantum states, which is not possible if the nucleons are identical particles.

The extracted angular distributions for the transition to the 7$^+$ state are presented in Fig. 6. The excitation-energy region of interest was fit with Gaussian peaks as described in Sec. III; however, at the widest angles, the transition to the 7$^+$ state completely dominates the spectra (see Figs. 1 and 2) and simple peak summing yields the same results. Note that at forward angles there is another state which cannot be separated from the 7$^+$ state because it appears at nearly the same excitation energy. This other state is presumably the known 2$^+$ state at $E_x = 1.14$ MeV, separated by only ~ 30 keV from the 7$^+$ state. The excitation of this other state is discussed more fully below. The wide-angle portion (from about 25°) is described well by a DWIA calculation for a transition to a 7$^+$ state as shown in Fig. 6. The DWIA calculation is entirely similar to the calculation described above for the 0$^+$, IAS transition except that the spin of the final state is indicated to be 7. Note that the calculated cross sections are dominated here by the tensor term of the nucleon-nucleon effective interaction. The normalizations required to make the calculations agree with the experimentally measured angular distributions are 0.60 at 135 MeV and 0.52 at 160 MeV. [The normalizations indicated in Fig. 6 use the 1f-2p shell-model wave functions described below and are $\sim 10\%$ higher than required assuming pure $(f_{7/2}, f_{7/2}^{-1})$ structure.]

It is important to realize that cross sections for the 7$^+$ transition are expected to be sensitive (i.e., in *first* order) to any correlations in the ground state of ^{48}Ca. Since the only way to form a 7$^+$ state in a one-step reaction is with the $(f_{7/2}, f_{7/2}^{-1})$ configuration, any part of the ^{48}Ca target nucleus which does not have the full strength of the eight excess neutrons in the $f_{7/2}$ shell, or a completely empty $f_{7/2}$ proton shell, will remove strength from this transition. Thus, the normalization factors required to make these calculations agree with the magnitude of the experimental cross sections are due, at least in part, to such

correlations in the ^{48}Ca target nucleus.

Although some normalization is required for this transition, it is noteworthy that the normalizations are significantly closer to unity than those required for similar comparisons of DWIA calculations with experimentally-measured cross sections for 1 $\hbar\omega$ stretched-state transitions observed in other nuclei. A normalization factor of about 0.31 to 0.37 is required for the (p,p'), (e,e'), and (p,n) excitation of the $T=1$, 4^- stretched state in ^{16}O and ^{16}F,[25,26,3] and of about 0.24 to 0.31 for the (p,p'), (e,e'), and (p,n) excitations of the $T=1$, 6^- stretched state in ^{28}Si and ^{28}P.[27–29] It is noteworthy that the hadronic inelastic-scattering normalization factors are about 20% smaller than the electron-scattering results.[28] This difference may indicate a need to decrease the strength of the isovector tensor term in the N-N effective interaction; the significant point here, however, is that all these normalization factors, whether from hadronic or electron scattering, are significantly smaller than the one we obtain for the 7^+ state transition, when analyzed in a similar fashion. Most of the difference between the normalization factors for the 1 $\hbar\omega$ transitions and that for the 0 $\hbar\omega$ transition in ^{48}Ca results from more ground-state correlations in ^{16}O and ^{28}Si than in ^{48}Ca; for example, Snover et al.[27] estimated the fractional occupancy of the $d_{5/2}$ orbital in ^{28}Si from the summed nucleon pickup strength to $\frac{5}{2}^+$ states in mass 27 to be 0.68. Thus, the inelastic-scattering normalizations actually indicate that the $(f_{7/2}, d_{5/2}^{-1})$ intensity of the $T=1$, 6^- state in $A=28$ is approximately $0.29/0.68 = 0.43$; however, Snover et al. present an analysis of their measured proton width of this state in ^{28}Si, based on the ^{27}Al(p,γ)^{28}Si and ^{27}Al(^{3}He,d)^{28}Si reactions, which indicates a $(f_{7/2}, d_{5/2}^{-1})$ intensity of the final state of about 0.7. This result is consistent also with the analysis of Halderson et al.[30] of the proton width of this state measured in low-energy ^{27}Al(p,p) elastic scattering. Thus, we have that the (p,p') and (e,e') normalizations for the excitation of the $T=1$, 6^- state in $A=28$ imply a $(f_{7/2}, d_{5/2}^{-1})$ intensity for the final state of only about 70% of that from the analyses of the proton width of this state in ^{28}Si.

A similar analysis for the $T=1$, 4^- states in $A=16$ can be attempted. This state is presumably dominated by the $(d_{5/2}, p_{3/2}^{-1})$ particle-hole configuration. The fractional occupancy of the $p_{3/2}$ neutron orbital in ^{16}O is approximately 0.88 from ^{16}O(p,d)^{15}O spectroscopic factors summarized by Roos et al.[31] Thus, the inelastic-scattering normalization factors indicate that the $(d_{5/2}, p_{3/2}^{-1})$ intensity of the $T=1$, 4^- state in $A=16$ is approximately $0.37/0.88 = 0.47$; however, a spectroscopic factor of 0.73 was obtained[32] from a DWBA analysis of the ^{17}O(d,t)^{16}O reaction proceeding to the 18.98 MeV, $T=1$, 4^- state, which indicates that this state, when formed as a neutron-particle, neutron-hole state, has a particle-hole intensity of at least 0.73. This result is consistent with the ^{15}N(p,γ)^{16}O study of this state by Snover et al.,[33] who observe a γ-decay rate from this state which is 0.7 ± 0.3 of that expected for a pure $(d_{5/2}, p_{3/2}^{-1})$ configuration. (Unfortunately, the uncertainty in the γ-decay rate is too large to determine the particle-hole intensity unambiguously.) Thus, again we have that the (p,p'), (p,n), and

(e,e') normalizations imply a particle-hole intensity for the final state significantly smaller than indicated by a transfer-reaction analysis. While the spectroscopic factors used in this analysis are probably not as reliable as for the analysis of the $T=1$, 6^- state in $A=28$ (mostly because there exist fewer measurements to provide consistency checks), the results are consistent in both cases.

The analysis of the excitation of the 7^+, 0 $\hbar\omega$ stretched state in the ^{48}Ca(p,n)^{48}Sc reaction can be attempted in a similar manner also. The fractional occupancy of the $f_{7/2}$ neutron orbital can be estimated from the 40-MeV ^{48}Ca(p,d)^{47}Ca measurements of Martin et al.[34] and the 25 MeV ^{48}Ca(^{3}He,^{4}He)^{47}Ca measurements of Fortier et al.,[35] who obtained spectroscopic factors for pickup strength to the $\frac{7}{2}^+$ ground state of 6.7 and 6.9, respectively. Thus, simply taking the average, we estimate that the fractional occupancy of the $f_{7/2}$ level in ^{48}Ca is about 0.85. Thus, the (p,n) normalization factor for the 7^+ transition of about 0.60 implies a $(f_{7/2}, f_{7/2}^{-1})$ particle-hole intensity of $0.60/0.85 = 0.71$. Unfortunately, it is not possible to measure directly the proton width of this state in ^{48}Sc, either by proton scattering or single-proton transfer reactions. (The 7^+ state has no analog in ^{48}Ca, and ^{47}Sc is unstable.) There does exist[4] some ^{48}Ca(^{3}He,t)^{48}Sc and ^{49}Ti(d,^{3}He)^{48}Sc data which show evidence for excitation of the 7^+ state, but do not provide the necessary spectroscopic information for the particle-hole strength. The (p,n) results reported here indicate that the particle-hole intensity of this state is large (viz., at least 70%) as indicated above. The results for the comparisons of the excitation of these isovector stretched states via inelastic-scattering experiments [viz., (e,e'), (p,p'), and/or (p,n)] with the nucleon-transfer experiments [viz., stripping, pickup, and/or (p,γ)] are presented in Table I for these three targets—^{16}O, ^{28}Si, and ^{48}Ca. One sees clearly that the (p,n) excitation of the 7^+ $(f_{7/2}, f_{7/2}^{-1})$ state in ^{48}Sc yields a considerably larger spectroscopic factor than that observed for the inelastic excitations of the 4^- and 6^- stretched states in mass 16 (^{16}O or ^{16}F) and mass 28 (^{28}Si or ^{28}P).

There exist several possible sources of the discrepancies observed between the stretched-state normalizations obtained from the various inelastic-scattering excitations and the transfer-reaction studies. There may exist ambiguities in the impulse-approximation descriptions which describe the inelastic-scattering reactions; for example, we find that if reasonable wine-bottle optical potentials[36] are used in the DWIA calculations for the (p,n) reaction, the stretched-state normalizations are increased by about the necessary 30%. Recall, as discussed earlier for the 0^+, IAS, such an increase would be essentially cancelled by a decrease from density-dependent effects; however, Kelly and Carr found[44] such effects to be significantly less for unnatural parity transitions, such as the 7^+-state transition considered here.

Although the discussions above regarding the stretched-state normalization factors try to take into account "first-order" core polarizations (via the correction for the estimated fractional occupancy of the original particle orbital), no attempt was made to correct for "second-order" polarization effects. These second-order effects involve a recoupling of the core polarizations in

TABLE I. Comparison of isovector "stretched-state" particle-hole intensities from inelastic-scattering reactions with nucleon-transfer reactions. Nomenclature is essentially that used in Ref. 27. $S(x,x')$ represents the inelastic scattering spectroscopic factor. V_h^2 represents fractional occupancy of hole-state orbital in target nucleus, A. S_{transfer} represents the nucleon transfer (or capture) spectroscopic factor. β_h^2 represents the one-hole intensity of the $A-1$ target nucleus.

Nucleus	State	$S(x,x')/V_h^2 \equiv S_i$	$S_{\text{transfer}}/\beta_h^2 \equiv S_t$	Ratio ($=S_i/S_t$)
^{16}O/^{16}F	4^- $(d_{5/2},p_{3/2}^{-1})$	$0.37^a/0.88^b=0.43$	$\sim 0.7^g$	0.64
^{28}Si/^{28}P	6^- $(f_{7/2},d_{5/2}^{-1})$	$0.29^c/0.68^d=0.47$	0.67^d	0.67
^{48}Ca/^{48}Sc	7^+ $(f_{7/2},f_{7/2}^{-1})$	$0.60^e/0.85^f=0.71$	<1.0	>0.71

^{a}References 3, 25, and 26.
^{b}Reference 31.
^{c}References 27–29.
^{d}Reference 27.
^{e}This work.
^{f}References 34 and 35.
^{g}Reference 32.

the final state [including $\nu f_{7/2} \rightarrow \pi f_{7/2}$ transitions induced by the (p,n) reaction for the ^{48}Ca(p,n)^{48}Sc case]. These recouplings have the effect of reducing the strength of the simple 1p-1h excitations by coupling to various other multiparticle, multihole states. (See, for example, the perturbation diagrams in the work of Towner and Khanna.[37]) Because these second-order polarization effects may occur during the particle-hole excitation, the pickup spectroscopic factors do not tell us anything about the size of these effects. These corrections will vary from target to target, and may be able to account for the ratios of inelastic-scattering spectroscopic factors to nucleon-transfer spectroscopic factors as listed in Table I.

The fact that the strengths of the stretched states are observed *both* in the inelastic-scattering experiments and in the nucleon-transfer experiments to be less than the simple theoretical estimates is due presumably to the combined effects of mesonic exchange currents and core polarization. For the 6^- stretched states in ^{28}Si, Amusa and Lawson[38] showed that, if one includes the $2s_{1/2}$ orbit in the shell-model description of the states of ^{28}Si, the inelastic scattering and stripping cross sections are reduced significantly. They indicate that if one were able to include also the $1d_{3/2}$ orbit (which is difficult to do because of the resulting size of the configuration space), one may be able to bring theory and experiment into reasonable agreement. We see similar results for the 7^+ state considered in this work if a $1f$-$2p$ shell-model calculation is used to describe ^{48}Ca and the 7^+ final state in ^{48}Sc. This calculation provides for *some* 2p-2h mixing with the predominant $(f_{7/2},f_{7/2}^{-1})$ configuration and reduces the predicted strength for this transition by 10%. (This structure calculation is described more fully below.) In summary, for the 7^+ state transition, we find a normalization factor that is significantly larger than those obtained for 1 $\hbar\omega$ stretched-state excitations when the DWIA analyses are performed in similar fashion. If one considers the available evidence for decreasing the strength of the isovector tensor term in the N-N effective interaction, the use of wine-bottle optical potentials, and the effects of core polarization and configuration mixing, the required normalization factor approaches unity; clearly, however, the am-

biguities of these effects and others make the final spectroscopic factor uncertain by at least $\pm 30\%$, similar to the IAS.

C. The 1^+–6^+ transitions

The 0^+, IAS and the 7^+ 0 $\hbar\omega$ stretched state are the lowest and highest spin members of the $(f_{7/2},f_{7/2}^{-1})$ octet of states. Now we proceed to consider the transitions to the other members of this band. These intermediate-spin members are all known[5,6] in ^{48}Sc. The state of highest excitation energy of the entire octet is the 0^+, IAS at $E_x=6.67$ MeV. The other states are observed to lie at lower and lower excitation energies as the spin increases, up to the 6^+ state, which is known[6] to be the ground state of ^{48}Sc. The last member of the band (the 7^+ state) is observed to lie at a higher excitation energy (viz., at $E_x=1.10$ MeV). This spectrum of excitation energies is well known.[5,6] The fact that the ground state is the next-to-highest spin member of the octet is a good example of one of the well-known Nordheim rules.[39] Basically, the higher spin states can have stronger residual interactions than the 0^+, IAS; however, the correlations between the particle and hole are minimized in the state with $J=j_h+j_p-1$.[40]

The intermediate-spin members of this band clearly seen in this experiment are the 1^+, 3^+, and 5^+ states. These states are indicated in the excitation-energy spectra of Figs. 1 and 2. The 2^+ member is probably observed, as discussed below, and the 4^+ and 6^+ states are excited only weakly in this reaction, also as discussed below. The structure of the intermediate-spin members of the octet is not uniquely the $(f_{7/2},f_{7/2}^{-1})$ configuration, even in the simple Tamm-Dancoff approximation (TDA), which assumes that the ^{48}Ca target nucleus is a pure $(\nu f_{7/2})^8$ configuration. Neutrons can be excited easily into the $2p_{3/2}$, $2p_{1/2}$, and $1f_{5/2}$ levels to form positive parity states with spins between 1 and 6. Only the 0^+, IAS and the 7^+ stretched state are pure $(f_{7/2},f_{7/2}^{-1})$ configurations within this (limited) basis. For the purposes of comparison here, we adopt a $1f$-$2p$ shell-model calculation which uses the two-body matrix elements of Van Hees and Glaudemans[47]

(hereafter referred to as the Utrecht interaction). The single-particle energies of the $1f$-$2p$ states are taken also from Van Hees and Glaudemans, except that the $f_{7/2}$-$f_{5/2}$ splitting was increased by 2 MeV in order to reproduce more accurately the observed 1^+ spectrum (see the companion paper on Gamow-Teller strength in this reaction). This modification probably is required because the Utrecht interaction was fit to known states in $A = 52$–55 nuclei and the spacings could be different near $A = 48$. The basis assumed is

$$(1f_{7/2})^8 + [(1f_{7/2})^7(1f_{5/2}, 2p_{3/2}, 2p_{1/2})] ,$$

which allows for 2p-2h states of the type where one of the particles must always be in the $f_{7/2}$ level. The (p,n) reaction picks out only the 1p-1h part of the final-state wave function, so only this part is used in the DWIA calculations. Although this is a truncated $1f$-$2p$ shell-model basis, it probably includes the most important class of 2p-2h configurations to describe states in $A = 48$ nuclei.

The comparison of the DWIA calculations with the measured angular distribution for the 1^+ state (at $E_x = 2.52$ MeV) is shown in Fig. 7. The calculations are essentially the same as those described above for the 0^+, IAS transition except that the structure assumed for the 1^+ state is taken from the modified Utrecht interaction. The calculations indicate that the transition is dominated by the central term of the nucleon-nucleon effective interaction. Normalization factors of 0.69 and 0.64 are required at 134 and 160 MeV, respectively, in order to make the calculations agree in magnitude with the experimental cross sections at forward angles. The result that these normalization factors differ by less than 10% (within the experimental uncertainties) indicates that the value of $V_{\sigma\tau}$ does not change significantly over this energy region. This result is consistent with the energy dependence of $V_{\sigma\tau}$ deduced from experimental studies[41,42] of the ^{12}C(p,n)^{12}N(1^+,g.s.) reaction from 100 to 200 MeV. The shape of the measured angular distribution is fit reasonably well out to the widest angle extracted of about 20°. (The experimental strength for this transition was extracted by peak fitting, as discussed in Sec. III.) The strength observed in this transition is discussed further in the companion paper on Gamow-Teller strength observed in this reaction. It is noteworthy that the DWIA calculations for

this transition are about five times larger if one assumes the structure to be described by a pure $(\pi f_{7/2}, \nu f_{7/2}^{-1})$ wave function rather than by the $1f$-$2p$ wave functions. See Table II.

The 2^+ and 7^+ states are known[6] to lie within 1.14 MeV of the (6^+) ground state. As discussed in Sec. III, the 0 to 1.1 MeV excitation-energy region was fit with Gaussian peaks in the time-of-flight spectra. The fitting procedure yielded three complexes, one from $E_x = 0.0$ to 0.25 MeV, one near $E_x = 0.6$ MeV, and one at $E_x = 1.1$ MeV. The complex between 0.0 and 0.25 MeV includes the 4^+, 5^+, and 6^+ states, known to be at $E_x = 0.252$, 0.131, and 0.00 MeV, respectively. The strength extracted near 0.6 MeV is presumably the transition to the 3^+ state at $E_x = 0.622$ MeV, and the strength near 1.1 MeV includes both the 2^+ and 7^+ transitions to the states known to be at 1.14 and 1.10 MeV, respectively. Let us consider the analysis of each of these complexes, in turn.

The experimental angular distribution for the 0.0 to 0.25 MeV complex is shown in Fig. 8. The angular distribution is seen to be peaked near 28°, consistent with that expected for a $\Delta l = 4$ transition. Both the 4^+ and 5^+ transitions would be expected to be dominated by $\Delta l = 4$ angular momentum transfers (the latter with spin transfer); the 6^+ transition would require $\Delta l = 6$, however, and would be expected to exhibit an angular distribution similar to that observed for the 7^+ transition, which is seen to be peaked near 37°. Although there appears to be some $\Delta l = 6$ strength required to fit the wide-angle part of the angular distribution, the dominant strength is clearly $\Delta l = 4$. Note that the 6^+ ground state should be resolvable from the 7^+ state at 1.1 MeV since the energy resolution is $\sim$450 keV; yet the 45° spectrum in Fig. 1 shows very little strength near the ground state compared to that observed for the 7^+ stretched state at 1.1 MeV. *The conclusion is that the 6^+ state is excited only weakly in this reaction.*

The weak excitation of the 6^+ state is entirely consistent with earlier predictions by Petrovich and Love[43] and also by Picklesimer and Walker[4] that transitions dominated by the tensor term of the nucleon-nucleon effective interaction will excite normal-parity transitions only via exchange processes, which are expected to be relatively weak. In fact, DWIA calculations (similar to those described above) predict that the 4^+ and 6^+ transitions

TABLE II. Normalization factors[a] required to make DWIA calculations agree in magnitude with the experimental measurements for the $(\pi f_{7/2}, \nu f_{7/2}^{-1})$ band in the ^{48}Ca(p,n)^{48}Sc reaction.

E_x (MeV)	J^π	N (134 MeV) $(\pi f_{7/2}, \nu f_{7/2})$	N (134 MeV) $(1f$-$2p)^b$	N (160 MeV) $(1f$-$2p)^b$
6.67	0^+	0.93	0.93	0.75
2.52	1^+	0.13	0.69	0.64
1.14	2^+	0.28	0.46	
0.62	3^+	0.26	0.45	
0.0–0.2	$4^+ + 5^+ + 6^+$	0.28	0.40	
1.10	7^+	0.60	0.65	0.57

[a]The normalization factors are uncertain by at least the overall combined experimental uncertainty of ±12% (see the text). There may be an additional subjective uncertainty which could be larger than the experimental uncertainty for the 2^+ and 3^+ states and for the $(4^+ + 5^+ + 6^+)$, complex (see the text).
[b]With the modified Utrecht interaction (see the text).

would have peak cross sections only about 20% and 7% as large as those for the 5^+ and 7^+ transitions, respectively. The angular distribution of Fig. 8 is consistent with these predictions. In Fig. 8, we show the separate and combined contributions from these three transitions, as calculated in the DWIA, all normalized by the *same* factor, viz., 0.40. The overall agreement with the observed shape is seen to be good. Note that while the 6^+ strength could not be significantly greater than that indicated, the amount of 4^+ strength vs 5^+ strength cannot be determined experimentally since they both should be primarily $\Delta l = 4$. The somewhat smaller normalization factor required probably indicates that these simple particle-hole wave functions are not as accurate for these transitions as for the stretched-state case. As indicated in Table II, the DWIA calculations for this complex are nearly twice as large if the states are assumed to be pure $(f_{7/2}, f_{7/2}^{-1})$.

The comparison of the angular distribution extracted for the strength near 0.6 MeV with the DWIA calculation for the transition to the 3^+ state is shown in Fig. 9. As indicated above, the wave function for the 3^+ state is taken from the $1f$-$2p$ shell-model calculations with the modified Utrecht interaction. The shape of the measured angular distribution, including the rise observed at $0°$ (which is due to the central term of the effective interaction), is described reasonably well by the calculations. The required normalization factor is 0.45, as compared with 0.24 if the state is assumed to be pure $(f_{7/2}, f_{7/2}^{-1})$.

The angular distribution for the strength observed near $E_x = 1.1$ MeV is shown again in Fig. 10. (It was shown earlier in Fig. 6.) The 2^+ state is known to be at $E_x = 1.14$ MeV and could not be resolved in this experiment from the 7^+ state at $E_x = 1.10$ MeV; however, since the transitions to these two states should involve $\Delta l = 2$ and 6, respectively, their angular distributions would be expected to peak at very different angles. In Fig. 6, we saw that the wide-angle part of this complex is described well by the DWIA calculation for the 7^+ transition. In Fig. 10, we show the comparison of the DWIA calculation for the 2^+ transition with this same measured angular distribution. Although the calculated angular distribution is peaked at a rather forward angle ($\sim 14°$), and would account for *much* of the strength observed at forward angles in this angular distribution, we see that the agreement is not really very good. Since the shapes of the 0^+, 1^+, 3^+, 5^+ (complex), and 7^+ transitions are all reproduced well by the DWIA calculations, it is hard to understand why the agreement is so poor for the 2^+ case. There is a state known at $E_x = 1.40$ MeV, which is tentatively identified[6] to be a 2^- state, and would be expected to exhibit a $\Delta l = 1$ angular distribution, in better agreement with the measured angular distribution; however, a state at $E_x = 1.40$ MeV is resolvable with the 320 keV resolution of this experiment, from the two states at $E_x = 1.10$ and 1.14 MeV. The centroid of this complex at forward angles is clearly observed to be at $E_x = 1.1$ MeV, and not at $E_x = 1.4$ MeV. Thus, the difficulty remains. Note also that the 160 MeV analysis presents this same problem. [The experimental angular distribution is shown in Fig. 6(b).]

One interesting, but speculative, possible explanation of

the observed shape of the 2^+ angular distribution is that a two-step Gamow-Teller process could be contributing significantly. Such a process would involve a (p,n) $0^+ \rightarrow 1^+$ transition, followed by a (n,n') $1^+ \rightarrow 2^+$ transition, and could be significant because of the strength of the GT term (i.e., $V_{\sigma\tau}$) in the effective interaction at these energies. Such a two-step process would be dominated by $\Delta l = 0$ transitions in each step. A combination of $\Delta l = 0$ and 2 angular distributions could easily explain the observed shape. Unfortunately, such a two-step process is beyond the scope of the DWIA calculations presented here, so that no definite conclusions can be made at this time. It is important to note that if such a two-step process is important here, it would be significant also in 0^+ to 0^+ transitions, and our present understanding of the V_τ strength in the effective interaction would be in error.

V. SUMMARY

The study of the ^{48}Ca(p,n)^{48}Sc reaction at medium energies tests both reaction-mechanism and nuclear-structure models. Because the ^{48}Ca target nucleus is described well by the simple shell model, and because the (p,n) reaction above about 100 MeV is predominantly an impulsive, one-step process, the ^{48}Ca(p,n)^{48}Sc reaction is dominated by simple transitions to one-particle, one-hole states which should be amenable to theoretical analyses. We observe strong excitations of several members of the known $(\pi f_{7/2}, \nu f_{7/2}^{-1})$ band of states in ^{48}Sc. We see the transitions to the 0^+, IAS (at 6.67 MeV), the 1^+ state (at 2.52 MeV), the 3^+ state (at 0.62 MeV), the 5^+ state (at 0.13 MeV), and the 7^+, 0 $\hbar\omega$ stretched state (at 1.10 MeV).

The 0^+, IAS transition at 134 MeV is described reasonably well by a DWIA calculation which assumes the 0^+ state is pure $(f_{7/2}, f_{7/2}^{-1})$. Basically, the calculation assumes complete overlap of the initial- and final-state wave functions, which is a good assumption for this (IAS) transition. That the magnitude of the cross sections are predicted by the DWIA with essentially no normalization factor indicates that the distorted-wave description, the assumed one-step, impulsive reaction mechanism, and the assumed strength of the isospin-transfer term in the nucleon-nucleon effective interaction are all reasonable—or that there is a fortuitous cancellation of two or more of these factors. Consideration of density-dependence effects on the N-N effective interaction and ambiguities in the optical-model parameters indicate that the latter situation is quite possible.

The transition to the 7^+, 0 $\hbar\omega$ stretched state is important because it addresses the structure of the ^{48}Ca target nucleus. The assumed $(f_{7/2}, f_{7/2}^{-1})$ structure of the 7^+ state is probably relatively accurate, since there exists no other one-particle, one-hole configurations which can produce such a state below 2 $\hbar\omega$ of excitation. A normalization factor of about 0.60 which is required for simple DWIA calculations for this transition increases to about 0.70 when configuration mixing in the f-p shell is taken into account with shell-model wave functions which include some of the possible 2p-2h configurations available. It is significant that the normalization factor required for the 7^+ stretched state is considerably larger than the normalization factors required for various 1 $\hbar\omega$ stretched-

state comparisons in several other nuclei, with analyses performed in similar fashion. The larger normalization factor required here is presumably a reflection of the fact that ^{48}Ca is a relatively good closed-shell nucleus, and that the final state is a relatively good 1p-1h state. If one considers the effects of the fractional occupancy of the $(\nu f_{7/2})$ orbital in ^{48}Ca, the observed normalization factor implies that the $(f_{7/2}, f_{7/2}^{-1})$ intensity of the final state is at least 70%. Consideration of other corrections, indicated by discrepancies observed for isovector 1 $\hbar\omega$ stretched-state transitions, likely will move this 1p-1h intensity even higher.

The other members of the $(f_{7/2}, f_{7/2}^{-1})$ band seen to be excited strongly in this reaction are the 1^+, 3^+, and 5^+ states. These excitations in the 135 MeV measurements were compared with the DWIA calculations, which use wave functions obtained from a truncated $1f$-$2p$ shell-model basis. The normalizations required to make these calculations agree in magnitude with the experimental results are 0.69, 0.45, and 0.40, respectively. It is noteworthy that we do not see strong excitations of the 4^+ or 6^+ members of the $(f_{7/2}, f_{7/2}^{-1})$ band, even though these states are known in ^{48}Sc. The 6^+ state is known to be the ground state of ^{48}Sc and is observed to be excited with less than 10% of the strength of the 7^+ stretched state. The weak excitation of these two states is due apparently to the fact that transitions dominated by the tensor term of the nucleon-nucleon effective interaction are expected to

be able to excite normal parity states only via exchange processes, which are predicted to be weak.

The one remaining member of the $(f_{7/2}, f_{7/2}^{-1})$ octet is the 2^+ state known to be at $E_x = 1.14$ MeV. Presumably we see this state at forward angles unresolved from the 7^+ state at 1.10 MeV; however, the angular distribution observed for this transition is not described well by a DWIA calculation, assuming $\Delta l = 2$, as expected. The observed shape of this angular distribution could be described by a combination of $\Delta l = 0$ plus $\Delta l = 2$ and may indicate two-step contributions to this transition.

In conclusion, the ^{48}Ca(p,n)^{48}Sc reactions at 135 and 160 MeV exhibit strong transitions to several states at low excitation energies which are believed to be dominated by the $(\pi f_{7/2}, \nu f_{7/2}^{-1})$ particle-hole structure. The generally good agreement between the measured angular distributions and DWIA calculations with $1f$-$2p$ shell-model wave functions supports this interpretation and indicates that the (p,n) reaction at medium energies is a good probe of 1p-1h strength.

[1]B. D. Anderson, J. N. Knudson, P. C. Tandy, J. W. Watson, R. Madey, and C. C. Foster, Phys. Rev. Lett. **45**, 699 (1980).

[2]C. D. Goodman, C. A. Goulding, M. B. Greenfield, J. Rapaport, D. E. Bainum, C. C. Foster, W. G. Love, and F. Petrovich, Phys. Rev. Lett. **44**, 1755 (1980).

[3]A. Fazely, B. D. Anderson, M. Ahmad, A. R. Baldwin, A. M. Kalenda, R. J. McCarthy, J. W. Watson, R. Madey, W. Bertozzi, T. N. Buti, J. M. Finn, M. A. Kovash, B. Pugh, and C. C. Foster, Phys. Rev. C **25**, 1760 (1982).

[4]A. Picklesimer and G. E. Walker, Phys. Rev. C **17**, 237 (1978).

[5]H. Ohnuma, J. R. Erskine, J. P. Schiffer, J. A. Nolen, and N. Williams, Phys. Rev. C **1**, 496 (1970); H. Ohnuma and J. L. Yutema, *ibid.* **2**, 1725 (1970).

[6]*Nuclear Level Schemes, A=45 through A=257*, edited by Nuclear Data Group (Academic, New York, 1973).

[7]C. D. Goodman, C. C. Foster, M. B. Greenfield, C. A. Goulding, D. A. Lind, and J. Rapaport, IEEE Trans. Nucl. Sci. NS-26, 2248 (1979).

[8]J. W. Watson, M. Ahmad, B. D. Anderson, A. R. Baldwin, A. Fazely, P. C. Tandy, R. Madey, and C. C. Foster, Phys. Rev. C **23**, 2373 (1981).

[9]R. Madey, J. W. Watson, M. Ahmad, B. D. Anderson, A. R. Baldwin, A. L. Casson, W. Casson, R. A. Cecil, A. Fazely, J. N. Knudson, C. Lebo, W. Pairsuwan, R. J. Pella, J. C. Varga, and T. R. Witten, Nucl. Instrum. Methods **214**, 401 (1983).

[10]A. R. Baldwin and R. Madey, Nucl. Instrum. Methods **197**, 379 (1982).

[11]R. Cecil, B. D. Anderson, and R. Madey, Nucl. Instrum. Methods **161**, 439 (1979).

[12]N. R. Stanton, Ohio State University Report No. COO-1545-92, 1971.

[13]M. W. McNaughton, N. S. P. King, F. P. Brady, and J. L.

Ullman, Nucl. Instrum. Methods **129**, 241 (1975).

[14]F. P. Brady and J. R. Romero, Crocker Nuclear Laboratory Progress Report UCD-CNL 192, 1979; and (private communication).

[15]B. D. Anderson, J. N. Knudson, R. Madey, and C. C. Foster, Nucl. Instrum. Methods **169**, 153 (1980).

[16]J. W. Watson, B. D. Anderson, A. R. Baldwin, C. Lebo, B. S. Flanders, W. Pairsuwan, R. Madey, and C. C. Foster, Nucl. Instrum. Methods **215**, 413 (1983); J. D'Auria *et al.*, Phys. Rev. C **30**, 1999 (1984).

[17]G. L. Moake, L. J. Gutay, R. P. Scharenberg, P. T. Debevec, and P. W. Quin, Phys. Rev. Lett. **43**, 910 (1979).

[18]P. R. Bevington, K. G. Kibler, and B. D. Anderson, Case Western Reserve University Report No. COO-1573-63, 1969 (unpublished); P. R. Bevington, *Data Reduction and Error Analysis for the Physical Sciences* (McGraw-Hill, New York, 1969), p. 237.

[19]F. Osterfeld, Phys. Rev. C **26**, 762 (1982).

[20]J. Raynal and R. Schaeffer, computer code DWBA 70. The version we used was supplied to us by W. G. Love.

[21]P. Schwandt, H. O. Meyer, W. W. Jacobs, A. D. Bacher, S. E. Vigdor, M. D. Kaitchuck, and T. R. Donoghue, Phys. Rev. C **26**, 55 (1982).

[22]W. G. Love and M. A. Franey, Phys. Rev. C **24**, 1073 (1981).

[23]B. A. Brown, C. F. Clement, and S. M. Perez (unpublished); and (private communication).

[24]T. N. Taddeucci, J. Rapaport, D. E. Bainum, C. D. Goodman, C. C. Foster, C. Gaarde, J. Larsen, C. A. Goulding, D. J. Horen, T. Masterson, and E. Sugarbaker, Phys. Rev. C **25**, 1094 (1981).

[25]R. S. Henderson, B. M. Spicer, I. D. Svalbe, V. C. Officer, G. G. Shute, D. W. Devins, D. L. Friesel, W. P. Jones, and A. C.

Attard, Aust. J. Phys. **32**, 411 (1979).

[26]S. Yen, R. J. Sobie, T. E. Drake, A. D. Bacher, G. T. Emery, W. P. Jones, D. W. Miller, C. Olmer, P. Schwandt, W. G. Love, and F. Petrovich, Phys. Lett. **105B**, 421 (1981).

[27]K. A. Snover, G. Feldman, M. M. Hindi, E. Kuhlmann, N. N. Harakeh, M. Sasao, M. Noumachi, Y. Fujita, M. Fujiwara, and K. Hosono, Phys. Rev. C **27**, 493 (1983).

[28]R. Lindgren and F. Petrovich, in *Spin Excitations in Nuclei,* edited by F. Petrovich *et al.* (Plenum, New York, 1984), p. 323.

[29]A. Fazely, R. Madey, B. D. Anderson, A. R. Baldwin, C. Lebo, J. W. Watson, W. Bertozzi, T. Buti, M. Finn, C. Hyde, J. Kelly, B. Pugh, and C. C. Foster, Bull. Am. Phys. Soc. **27**, 629 (1982).

[30]D. Halderson, K. W. Kemper, J. D. Fox, R. O. Nelson, E. G. Bilpuch, C. R. Westerfeldt, and G. E. Mitchell, Phys. Rev. C **24**, 786 (1981).

[31]P. G. Roos, S. M. Smith, V. K. C. Cheng, G. Tibell, A. A. Cowley, and R. A. J. Riddle, Nucl. Phys. **A255**, 187 (1975).

[32]G. Mairle, G. J. Wagner, P. Doll, K. T. Knopfle, and H. Bruer, Nucl. Phys. **A299**, 39 (1978).

[33]K. A. Snover, E. G. Adelberger, P. G. Ikossi, and B. A. Brown, Phys. Rev. C **27**, 1837 (1983).

[34]P. Martin, M. Beunerd, Y. Dupont, and M. Chabre, Nucl. Phys. **A185**, 465 (1972).

[35]S. Fortier, E. Hourani, M. N. Rao, and S. Gales, Nucl. Phys. **A311**, 324 (1978).

[36]These calculational tests were performed at 181 MeV using DWBA 70 with the wine-bottle optical-model parameters for ^{40}Ca reported by G. R. Satchler, Nucl. Phys. **A394**, 349 (1982).

[37]I. S. Towner and F. C. Khanna, Nucl. Phys. **A399**, 334 (1983).

[38]A. Amusa and R. D. Lawson, Phys. Rev. Lett. **51**, 103 (1983).

[39]L. W. Nordheim, Phys. Rev. **78**, 294 (1950); Rev. Mod. Phys. **23**, 322 (1951); and further elaborated by M. H. Brennan and A. M. Bernstein, Phys. Rev. **120**, 927 (1960).

[40]See, for example, G. F. Bertsch, *The Practitioner's Shell Model* (American Elsevier, New York, 1972), Chap. 5.

[41]J. Rapaport, T. Taddeucci, C. Gaarde, C. D. Goodman, C. C. Foster, C. A. Goulding, D. Horen, E. Sugarbaker, T. G. Masterson, and D. Lind, Phys. Rev. C **24**, 335 (1981).

[42]B. D. Anderson, R. J. McCarthy, M. Ahmad, A. Fazely, A. M. Kalenda, J. N. Knudson, J. W. Watson, R. Madey, and C. C. Foster, Phys. Rev. C **26**, 8 (1982).

[43]F. Petrovich and W. G. Love, Nucl. Phys. **A354**, 499c (1981).

[44]J. Kelly and J. A. Carr, in *Spin Excitations in Nuclei,* edited by F. Petrovich *et al.* (Plenum, New York, 1984), p. 253.

[45]N. Auerbach, J. D. Bowman, M. A. Franey, and W. G. Love, Phys. Rev. C **30**, 736 (1984).

[46]F. A. Brieva and J. R. Rook, Nucl. Phys. **A291**, 299 (1977); H. V. von Geramb (unpublished).

[47]A. G. M. van Hees and P. W. M. Glaudemans, J. Phys. A **303**, 267 (1981).